ARTICLE

Unraveling Interactions and Catalytic Mechanisms of Ionic Liquid [Bmim][BF_4] and Styrene Oxide Using Sum Frequency Spectroscopy†

Dujuan Meng[a], Linyu Han[a,b], Caihe Liu[a,b], Yuening Zhang[a], Xujin Qin[a,b], Yu Bai[a], Yuan Guo[a,b], Zhen Zhang[a,b*]

a. Beijing National Laboratory for Molecular Sciences, CAS Research/Education Center for Excellence in Molecular Sciences, Institute of Chemistry, Chinese Academy of Sciences, Beijing 100190, China
b. University of Chinese Academy Sciences, Beijing 100049, China

(Dated: Received on January 6, 2024; Accepted on February 7, 2024)

The utilization of ionic liquids as versatile reaction media and catalysts has garnered significant attention in the field of green and sustainable chemistry. In this study, sum frequency generation vibrational spectroscopy (SFG-VS) is employed to investigate the interactions between 1-butyl-3-methylimidazolium tetrafluoroborate ([Bmim][BF_4]) and styrene oxide (SO) at the air/liquid interface. Spectral analysis in the range of 1000 cm^{-1} to 3700 cm^{-1} reveals that only vibrational modes of C–H bonds are observed. Notably, the orientation of the epoxy ring of SO is found to be towards the bulk phase, while the three C–H groups on the imidazolium ring of the cation are parallel to the surface. Consequently, there are no observed interactions between the cation and SO. However, in the vibrational spectra of C–H bonds, interactions between the anion BF_4^- and the CH_2 group of the epoxy ring result in blue shifts in the vibrations of CH (SO) and CH_3 (cation). These findings support a proposed reaction mechanism where the ionic liquid catalyzes SO first and subsequently reacts with CO_2, providing valuable insights into intermolecular interactions and molecular orientations at reaction interfaces.

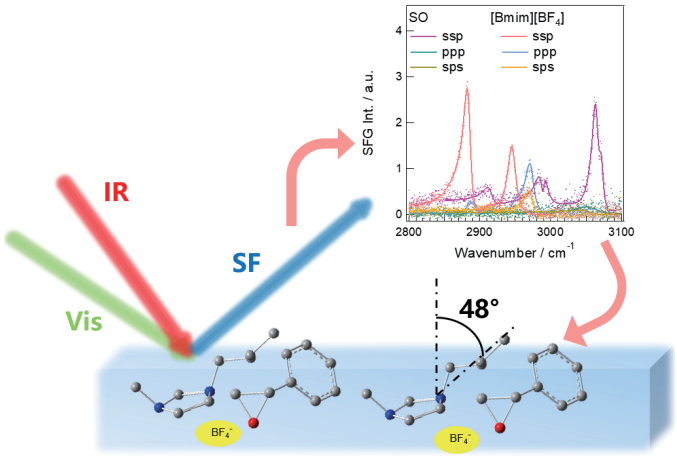

Key words: Sum frequency generation, Ionic liquid, Molecular interaction, Catalytic mechanisms

I. INTRODUCTION

Ionic liquids (ILs) have gained significant attention in recent years due to their remarkable properties and versatility in various chemical processes, particularly within the realm of green chemistry [1–5]. Their unique ability to serve as solvents and catalysts has led to extensive exploration of their potential applications. The chemical conversion of CO_2 into more valuable carbon-based energy and materials is an important way to effectively mitigate climate problems and promote the development of green energy. IL has more advantages and

† Part of Special Issue "In Memory of Prof. Qihe Zhu on the occasion of his 100th Anniversary".

* Author to whom correspondence should be addressed. E-mail: zhangz@iccas.ac.cn

 © 2024 Chinese Physical Society

prospects as a green catalyst than other materials, making it a natural choice for a wide range of applications in this field.

Among the ILs studied for designing catalysts in the chemical conversion reaction of CO_2, 1-butyl-3-methylimidazolium tetrafluoroborate is one that has been extensively studied [6–8]. There are three hypothesized reacting routes in the hypothesized mechanism. Shown in FIG. 1, the IL reacts with epoxide (styrene oxide) to open the oxide ring with the following addition of CO_2 to form cyclic carbonate ester (Route I), or the IL activates CO_2 and forms carbonate anion to react with epoxide (Route II), or both routes occur simultaneously. Braunschweig and co-workers have studied the electro-catalytic process of CO on the interface of Pt and IL using SFG-VS. The studies showed the importance of IL structures [C_2C_1im][BF_4] [9], [C_2C_1im][NTf_2] [10], and [C_4C_1Pyrr][NTf_2] [11] in electro-catalysis of CO via analyzing the changes of CO vibrational peak position and intensity with the potential and water content [12]. However, the catalytic molecular mechanism of this ionic liquid remains to be further studied [13–15].

Here, we used the SFG-VS to study the role of [Bmim][BF_4] in the reaction between styrene oxide (SO) and carbon dioxide (CO_2). Our findings reveal that the epoxy ring of SO is oriented towards the bulk phase, while the C–H groups on the imidazolium ring of the $[Bmim]^+$ cation align parallel to the surface. The vibrational spectra of C–H bonds expose significant interactions between the BF_4^- anion and the CH_2 group within the epoxy ring, resulting in distinct blue shifts in the vibrations of CH (SO) and CH_3 (cation).

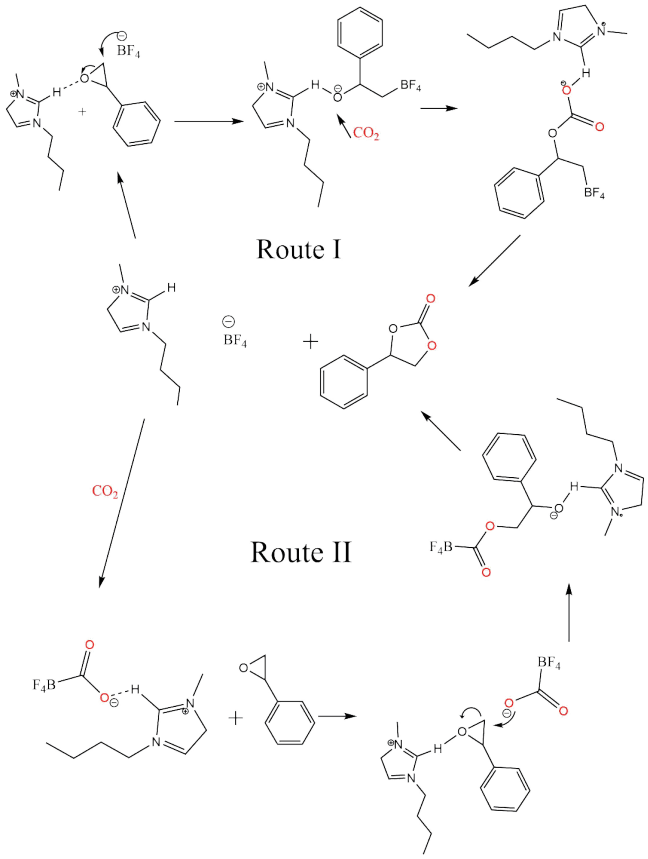

FIG. 1 Schematic of ionic liquid catalytic mechanism in CO_2 cyclic addition with styrene oxide.

II. EXPERIMENTS

The ionic liquid [Bmim][BF_4] (99%), styrene oxide (SO, 98%), and *N*,*N*-dimethyl formamide (DMF, 98%) were purchased from Sigma Aldrich and used without additional purification. Binary mixtures of [Bmim][BF_4]/SO, [Bmim][BF_4]/DMF, and SO/DMF with varying mole fractions ranging from 0% to 100% were prepared.

The setup for sum frequency generation vibrational spectroscopy (SFG-VS) is extensively described in the literatures [16–24]. Briefly, a femtosecond laser passed through an OPA and DFG system, generating tunable IR pulses with a center wavelength of 3440 nm. A picosecond laser with a pulse width 30 ps and wavelength 800 nm served as the visible (Vis) pulse. The two beams were electronically synchronized. Both the visible and IR beams overlap spatially and temporally at the sample, with incidence angles of 55° and 45°, respectively. Each SFG spectrum was captured using a monochromator (Andor SR-3231) and EMCCD (Newton DU970P 1600×200). The spectra were acquired for 10 min with the IR power of 6.7 mW and Vis power of 200 mW across all ranges of wavelengths. All spectra were normalized to the non-resonant SFG-VS of a *Z*-cut quartz crystal surface.

III. RESULTS AND DISCUSSION

The [Bmim][BF_4] and SO mixtures were investigated in a specific range of the SFG spectra (1000–3700 cm^{-1}) to determine if there were any interactions between the ions and molecules. Specifically, we have looked for the formation of hydrogen bond (3000–3600 cm^{-1}) between C(2)–H and the oxygen atom on SO, the presence of an epoxy ring (1280–

DOI: 10.1063/1674-0068/cjcp2401001 © 2024 Chinese Physical Society

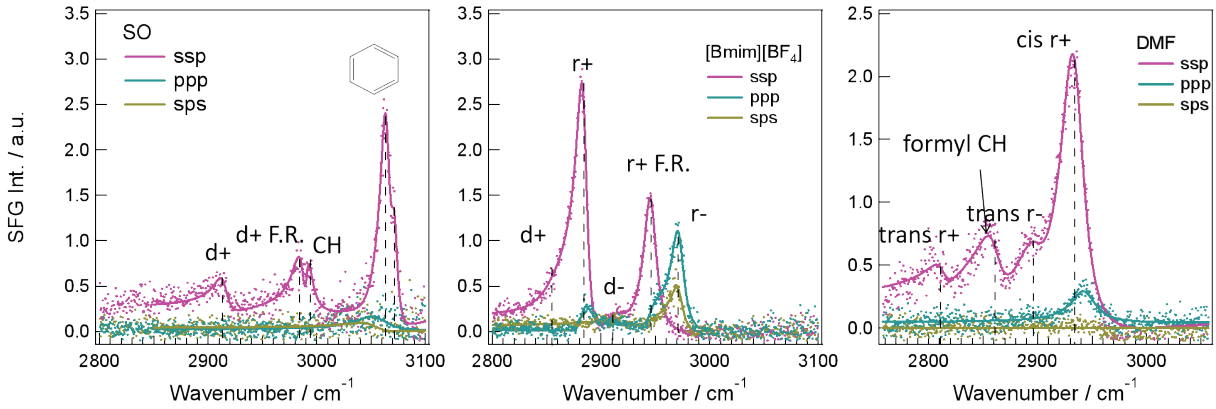

FIG. 2 Sum frequency spectra of styrene oxide (SO), ionic liquid [Bmim][BF_4], and *N,N*-dimethyl formamide (DMF) with combined polarizations (SF, Vis, IR) ssp, ppp, and sps.

1240 cm^{-1}), and any interactions between the anion (1000–1200 cm^{-1}) and epoxy ring. However, upon analyzing the results of [Bmim][BF_4] and SO mixtures, only vibrational spectra related to CH vibrations at 2800–3100 cm^{-1} and CH bending at 1350–1600 cm^{-1} were observed. Since cyclic C–O bonds in the epoxy ring are both IR and Raman active (FIG. S2 in Supplementary materials, SM), the absence of vibrational peaks in the spectra between 1100–1400 cm^{-1} indicates that the O in the epoxy ring is oriented toward the bulk phase-for two reasons. One reason is that we observed the SFG spectra of the O-CH rocking mode on the epoxy ring (~1390 cm^{-1}), indicating that the epoxy ring is not parallel to the surface (FIG. S2 in SM); the other reason is that we also observed the SFG spectra of the symmetrical stretching mode of CH on the benzene ring, which further demonstrates that the benzene ring is not parallel to the surface. Simultaneous measurements were conducted on the binary mixtures of [Bmim][BF_4]/DMF and SO/DMF. The purpose was to understand the solvation dynamics and compare the interaction behaviors with those observed in [Bmim][BF_4]/SO mixtures. The study provides essential insights into the interplay of intermolecular forces at the air/liquid interface.

A. SFG spectra of pure liquids

FIG. 2 illustrates the SFG spectra of the neat ionic liquid [Bmim][BF_4], SO, and DMF at the air/liquid interface. The vibrational peaks in the spectra are identified based on the selection rules of SFG spectra [18, 20]. For the SO molecule, the peaks observed at approximately 2915, 2986, and 2996 cm^{-1} correspond to the symmetric vibration of the CH_2 group, the CH_2 Fermi resonance (F.R.), and the CH stretching in the epoxy ring of SO. The peaks detected at 3050, 3064, and 3071 cm^{-1} originate from the vibrational modes associated with benzene ring, specifically ν_7, ν_{20a}, and ν_2, respectively [25–27]. In terms of [Bmim][BF_4], peak assignments to: a peak at 2853 cm^{-1} corresponding to the symmetrical stretching (ss) of CH_2-ss, a peak at 2884 cm^{-1} corresponding to the symmetrical stretching of CH_3 (CH_3-ss) for butyl chain, a peak at around 2916 cm^{-1} corresponding to CH_2-ss F.R., another one located at 2945 cm^{-1} which represents CH_3-ss F.R., and finally a peak at 2971 cm^{-1} corresponding to CH_3 as of IL-water mixtures [23, 28, 29] and IL alone [30–34]. The spectra of DMF exhibit the symmetric and asymmetric stretches for the *trans*-methyl group at 2813 and 2895 cm^{-1}, respectively.

The stretch of formyl CH is at 2863 cm^{-1}, and the symmetric stretch of the *cis*-methyl group is at 2937 cm^{-1}, showing relatively strong intensities in ssp and ppp spectra (FIG. 3) [35–37]. Given the pronounced peak intensities observed in ssp polarization combination spectra, we can compare the ssp spectra of binary mixtures with different mole fractions to elucidate intermolecular interactions. The spectra of the mixtures of SO/DMF and [Bmim][BF_4]/DMF are illustrated in FIG. 3 (b) and (c), respectively. No notable shifts in peak positions are observed as the mole fraction varies. Conversely, within the spectra of [Bmim][BF_4]/SO mixtures, we observe blue shifts in the IL-CH_3-ss mode (FIG. 3(a)) and SO-CH-str mode (FIG. 3(f)) with increasing concentration of [Bmim][BF_4]. Furthermore, the shifts of the peaks show a linear correlation with the concentration, as shown in FIG. 3(g), indicating that there are the strong interac-

DOI: 10.1063/1674-0068/cjcp2401001 © 2024 Chinese Physical Society

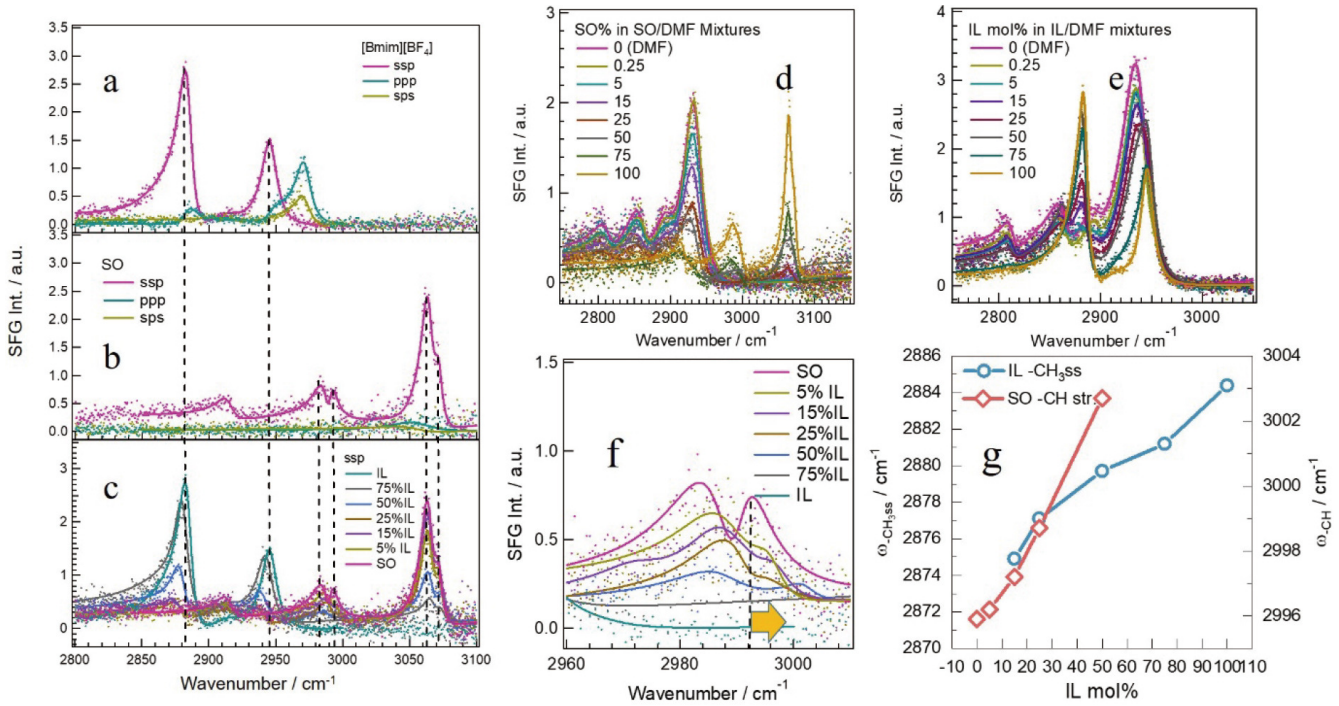

FIG. 3 ssp spectra of (a) [Bmim][BF$_4$]/SO mixtures, (b) SO/DMF mixtures, and (c) [Bmim][BF$_4$]/DMF mixtures. (d) ssp spectra of SO in SO/DMF mixtures at 2960–3020 cm^{-1}. (e) ssp spectra of [Bmim][BF$_4$]/DMF mixtures at 2960–3020 cm^{-1}. (f) ssp spectra of [Bmim][BF$_4$]/SO mixtures at 2960–3020 cm^{-1}. (g) The changes of vibrational peak positions for IL-CH$_3$ ss mode and SO-CH str mode.

tions between the ions and SO molecules.

B. Orientational analysis and surface density

To quantitatively analyze the concentration-dependence spectra, we employed a global fitting method, and the parameters can be found in SM. The molecule's tilt angle (θ) on the surface, when using a delta-distribution function, is determined by comparing the calculated intensity curves $\chi^{(2)}_{ppp}/\chi^{(2)}_{ssp}$ with the experimental intensity ratio. In this analysis, we employed the ratio A_{ppp}/A_{ssp} [23, 28, 38–40] to analyze the orientation of ions and molecules at the surface. The interfacial refractive index n' is calculated with the modified Lorentz model [41, 42]. The tilt angle of terminal methyl group on butyl chain in cation is 48°±1°, which is consistent with the literature value 47°±2° [23, 31]. The orientation of imidazolium ring in ionic liquids has been well-explained by Badeli [31–33]. The absence of N–CH$_3$, C(2)–H, and H–C(4)C(5)–H vibrational peaks in spectra suggests that the imidazolium ring is parallel to the surface plane. Applying the same calculation to DMF, we determined that the tilt angle of *cis*-CH$_3$ is 50.2°±1° with respect to the surface normal. However, the method used is not suitable for calculating the tilt angle of the phenyl ring in styrene oxide. This is because one of the vibrational modes of the phenyl ring involves whole C–H bonds in the ring. In previous studies, the orientation of benzene has been analyzed using molecular dynamics (MD) simulation and quantum chemical calculations [25–27, 43, 44]. The results show that the phenyl ring is either tilted at 60° or 120° to the surface normal. We also calculated the orientations of [Bmim]$^+$ and DMF (Table S3 in SM). Table S2 in SM provides the refractive indices of the binary mixtures. To calculate the otientation angle, the ratio between the hyperpolarizability tensor elements of R has to be determined. Here, R value for [Bmim][BF$_4$] is 2.7 [23, 45]. For DMF, no depolarization ratio can be found in the literatures, so we choose the R values of methanol (1.7) [46], acetone (1.9) [47], acetonitrile (2.3) [32], and DMSO (2.3) [48] based on their molecular structures. In order to choose the proper value of R for DMF, FIG. 4(a) demonstrates the tilt angle θ with different R values for DMF in [Bmim][BF$_4$]/DMF mixtures. Based on the plots, we found that the value of 2.3 appears to be reasonable for the ratio of A_{ppp}/A_{ssp} at different ration of DMF/IL mixture, especially at the 75% IL solution interface. Therefore, here we use R value of 2.3 for DMF tilt angle calculation.

DOI: 10.1063/1674-0068/cjcp2401001 © 2024 Chinese Physical Society

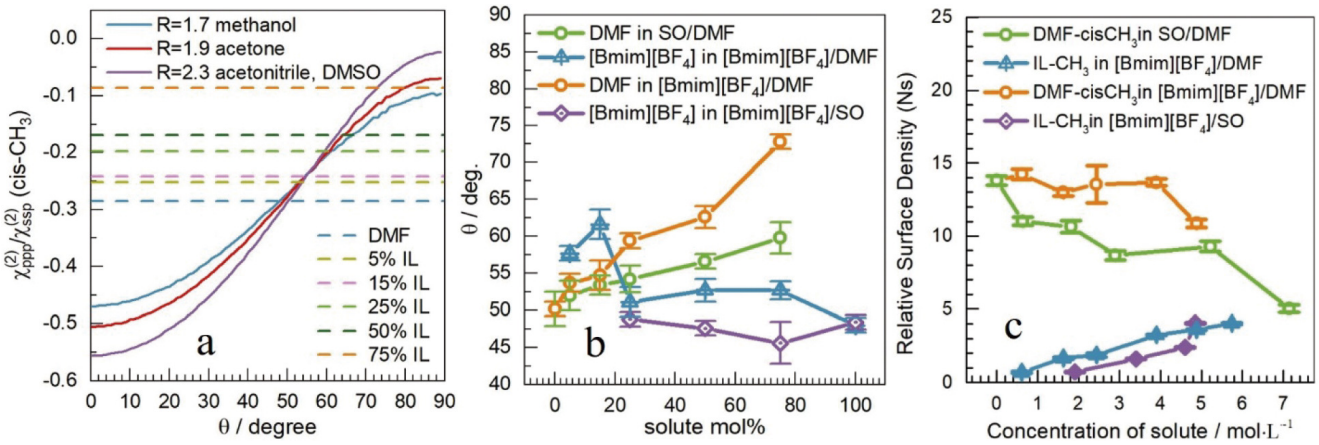

FIG. 4 (a) Orientational analysis CH_3-ss for DMF ss in [Bmim][BF_4]/DMF mixtures with different R values. (b) Tilt angle of the -CH_3 group on molecules of DMF in SO/DMF mixture (green scatters), [Bmim][BF_4] in [Bmim][BF_4]/DMF mixture (blue scatters), DMF in [Bmim][BF_4]/DMF mixture (orange scatters), and [Bmim][BF_4] in [Bmim][BF_4]/SO mixtures (purple sactters). (c) Relative surface density of molecule in mixtures depending on the bulk concentration of solute.

FIG. 4(b) presents the molecular orientations of [Bmim][BF_4] and DMF within various mixtures, namely [Bmim][BF_4]/SO, SO/DMF, and [Bmim][BF_4]/DMF. In the mixtures of SO/DMF and [Bmim][BF_4]/DMF, the orientation angle (θ) of the DMF-*cis*-CH_3 group increases with the addition of SO or [Bmim][BF_4]. This means when either SO or [Bmim][BF_4] is added, the DMF molecule attends to align parallelly to the surface plane. By comparing the orientation change when adding SO or [Bmim][BF_4], the tilt angle of DMF in [Bmim][BF_4] solution is larger than that in SO. As the orientation angle of imidazolium ring is parallel to the surface plane, such larger title angle change indicates a stronger interaction between DMF and [Bmim][BF_4] compared to DMF and SO. This observation aligns with molecular structure considerations, as interactions between DMF and SO primarily occur between the acyl group and the epoxy ring. However, interactions between [Bmim][BF_4] and DMF involve multiple interaction sites, including the acyl group with the imidazolium ring and interactions between the methyl group of DMF and the anions [49, 50]. Furthermore, the angle (θ) of the methyl group in the butyl chain of $[Bmim]^+$ shows a decreasing trend with an increasing mole percentage of [Bmim][BF_4] in [Bmim][BF_4]/DMF mixtures. In the [Bmim][BF_4]/SO mixtures, the angle (θ) appears to remain constant regardless of the concentration of [Bmim][BF_4]. As previously elucidated in studies by Wang and co-workers [51], the SF susceptibility is a function of the surface density N_s and the orientational angle θ following the equation:

$$\chi^{(2)}_{\text{eff}} = N_s \cdot d \cdot r(\theta) \tag{1}$$

At a given experimental configuration, the susceptibility strength factor d is a constant and the orientational field functional $r(\theta)$ contains all orientational information (see SM). Eq.(1) demonstrates that alterations in either N_s or θ result in a change in the peak amplitudes A_q. Given the value of θ and A_q, we can obtain relative values for N_s, which are plotted in FIG. 4(c) against the bulk concentration.

Before discussing the N_s of mixtures at surface, the A_q in mixtures' spectra as depicted in FIG. 5 are analyzed. Instead of using amplitude, we analyze the area of phenyl ring vibrations due to its unique characteristics. In FIG. 5(a), concerning the [Bmim][BF_4]/SO mixture, the A_q of IL-CH_3-ss mode and SO-CH mode demonstrates a linear correlation with the mole percent of [Bmim][BF_4]. Moving on to FIG. 5(b), we compare the area change of phenyl ring C–H modes with the amplitude change of phenyl ring ν_{20a} mode. They exhibit a similar trend in response to the mole percent of [Bmim][BF_4], with the area change showing better linearity, except for the 5% mixture. The anomaly at 5% suggests that strong interactions occurred between SO and $[Bmim]^+$, resulting in abnormal changes in N_s or θ. In the case of SO/DMF mixtures, the A_q of DMF-CH_3 and the area of phenyl ring modes also exhibit linear changes with SO% along with the A_q of IL-CH_3-ss and DMF-CH_3-ss modes in [Bmim][BF_4]/DMF mixtures (as observed in FIG. 5(c) and FIG. 5(d)).

The obtained surface density N_s can be described using the classical Langmuir model as shown in FIG. 6,

DOI: 10.1063/1674-0068/cjcp2401001 © 2024 Chinese Physical Society

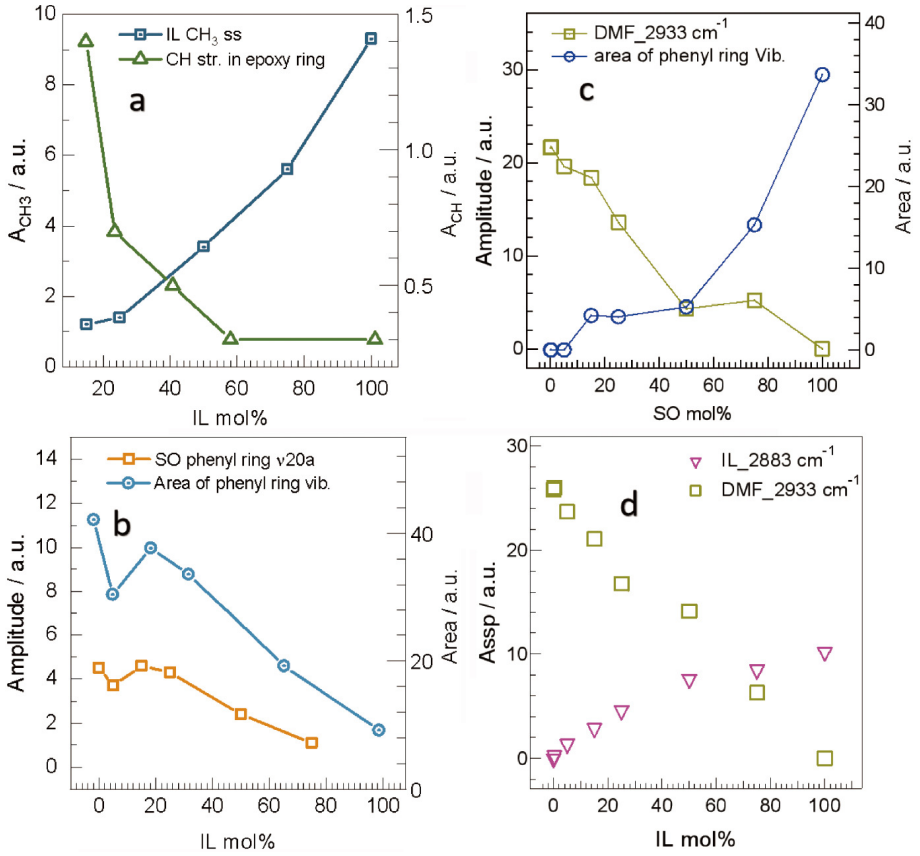

FIG. 5 (a) Changes of amplitudes of CH_3-ss mode and CH-str mode versus the concentration of IL in [Bmim][BF_4]/SO mixture. (b) The IL concentration dependence of the area of phenyl ring vibrations and the amplitude of ν_{20a} vibration mode of phenyl ring in [Bmim][BF_4]/SO mixture. (c) The amplitude change of DMF-CH_3-ss mode and area change of phenyl vibrations in SO/DMF mixture. (d) Changes of amplitudes of IL-CH_3-ss mode and DMF-CH_3-ss mode against the mole percent of IL in [Bmim][BF_4]/DMF mixture.

then we are able to determine the Gibbs free energy of adsorption, denoted as $\Delta G^0_{\rm ads}$ [52, 53].

$$N_{\rm s} = \frac{N_{\rm s}^{\rm max} C}{C + M\exp(\Delta G^0_{\rm ads}/RT)} \tag{2}$$

There, $N_{\rm s}^{\rm max}$ is the maximum obtainable surface number density, C is the bulk concentration of solute, M is the molarity of solvent, R is the ideal gas constant, and T is the thermodynamic temperature in K. We used Eq.(2) to fit the $N_{\rm s}$ (FIG. 6) and obtained the $\Delta G^0_{\rm ads}$ value of −0.51±0.08 kJ/mol for $[{\rm Bmim}]^+$, which is significantly smaller than the $\Delta G^0_{\rm ads}$ value of −12.6± 1.1 kJ/mol for aqueous [Bmim][MS] [23]. According to the Gibbs adsorption equation [52, 54], the interactions between ions and molecules are non-electrostatic and always attractive. A less negative $\Delta G^0_{\rm ads}$ value indicates lower bulk repulsion [53], which explains why DMF is a better solvent than water. The free energies of adsorption ($\Delta G^0_{\rm ads}$) for DMF in mixtures of [Bmim][BF_4]/DMF and SO/DMF are −6.08±0.76 kJ/mol and −0.95±0.32 kJ/mol, respectively. There is a higher repulsion between DMF and [Bmim][BF_4] compared to SO, which can be attributed to the hydrophobic interactions between the butyl chain and DMF. In the [Bmim][BF_4]/SO mixtures, the $\Delta G^0_{\rm ads}$ for [Bmim][BF_4] is 19.68±0.40 kJ/mol. However, this result is not valid due to the lack of $N_{\rm s}$ data at low concentrations (IL%<25%).

Based on the information presented, it becomes feasible to determine the reaction pathway for the catalysts involved in the chemical conversion of CO_2. The selection of route I over route II are substantiated by several key observations. Firstly, at the IL/SO solution interface, discernible shifts in the CH_3 SFG spectra correlated with solution concentration, in stark contrast to the consistent spectra observed at the IL/DMF solution interface. This phenomenon suggests that the observed shifts in peak positions predominantly stem from interactions between IL and SO molecules, rather than

DOI: 10.1063/1674-0068/cjcp2401001 © 2024 Chinese Physical Society

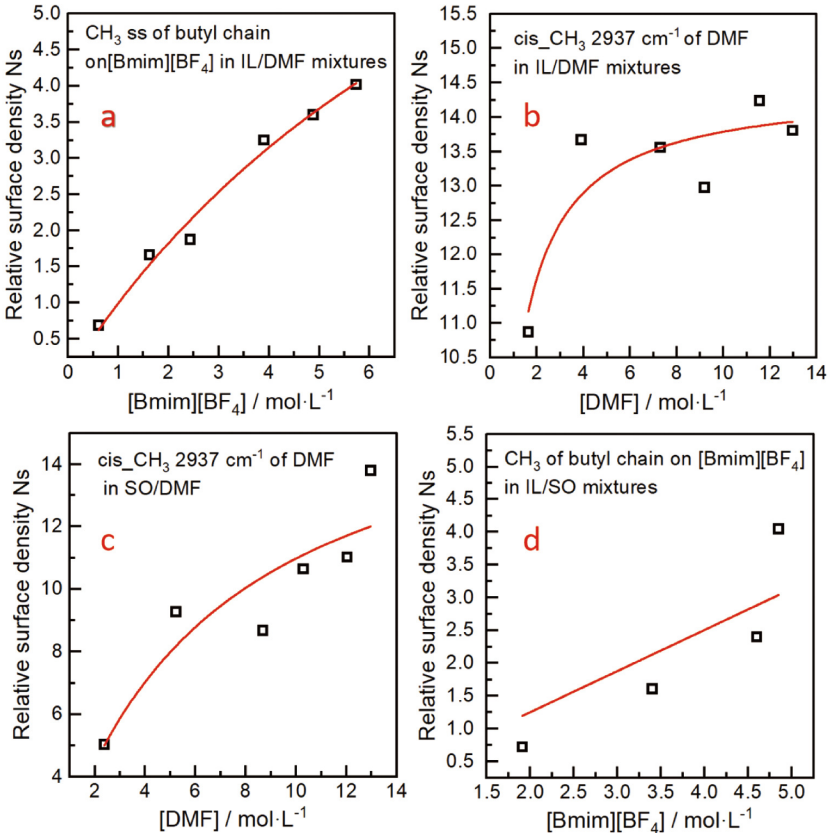

FIG. 6 The relative surface density, N_s *vs.* the solute concentrations in mixtures. (a) [Bmim][BF_4] in [Bmim][BF_4]/DMF mixture. (b) DMF in [Bmim][BF_4]/DMF mixture. (c) DMF in SO/DMF mixture. (d) [Bmim][BF_4] in [Bmim][BF_4]/SO. Red curves are the fits with Eq.(2).

variations in concentration. Moreover, the orientation angles and N_s values across different concentrations unveiled a remarkable consistency in the orientation angle of CH_3-IL at the IL/SO interface, irrespective of concentration fluctuations. Such consistency suggests the strong intermolecular interactions between IL and SO, thereby supporting the establishment of a comprehensive orientation diagram. Furthermore, the agreement between experimental outcomes and established literature findings supports the validity of route I. Specifically, this alignment with existing literature [31–34] regarding CO_2 behavior in IL environments implies either negligible reactivity or insufficient CO_2 concentration for reaction along route II, thus fortifying the basic principle for selecting route I for experimental investigations.

In summary, we have depicted the arrangement and interactions of the ionic liquid and styrene oxide in FIG. 7. In the ionic liquid, the terminal methyl group of the butyl chain is oriented towards the air, while the imidazolium ring is parallel to the surface plane. On the other hand, in the molecule of styrene oxide, the epoxy

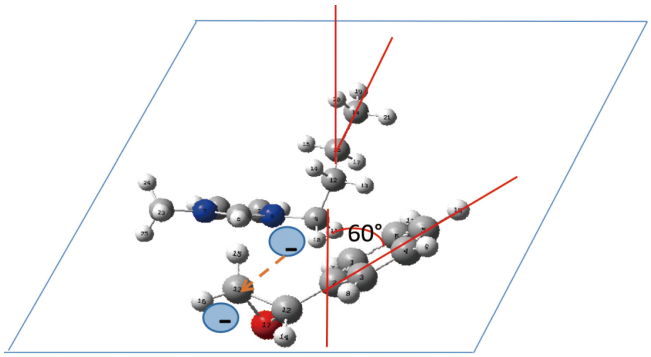

FIG. 7 Schematic of molecular orientations at air/liquid interface of [Bmim][BF_4]/SO mixtures.

ring points towards the bulk phase, and the phenyl ring is inclined at an angle of 60° to the surface normal. In our investigation, we examined the reaction mechanism depicted in route I (FIG. 1), where the anion BF_4^- interacts with the CH_2 group in styrene oxide. We expected to observe peak shifts of the CH_2 group (at 2916 cm^{-1}) in the spectra of the mixtures. However, we encountered a complication in the spectra of the mixtures due to the CH_2 Fermi resonance peak at 2916.8 cm^{-1} in the cation of $[Bmim]^+$. Therefore, we utilized the shift of the CH vibration in the epoxy ring

DOI: 10.1063/1674-0068/cjcp2401001 © 2024 Chinese Physical Society

to demonstrate the effects of the interactions in the mixtures. The presence of anions in the CH_2 (SO) group causes an increase in the electron density of the epoxy ring. This higher electron density leads to a stronger bond energy, resulting in a blue shift in the vibration of the CH group when ionic liquids are added. The shift in the vibration of the CH_3 groups in the butyl chain can also be explained by this interaction.

IV. CONCLUSION

In this study, we employed SFG-VS technique to investigate the interactions between [Bmim][BF_4] and SO, with the aim of gaining insight into the catalytic process by understanding ion-molecule interactions at the air/liquid interface. Spectral analysis was conducted in the range of 1000–3700 cm^{-1} to study the vibrations of chemical bonds, specifically focusing on C–H bonds. Our observations revealed that at the surface, the epoxy ring of SO is orientated toward the bulk phase, while the three C–H on the imidazolium ring of the cation are parallel to the surface. Consequently, no interactions were observed between cation and SO. However, in the vibrational spectra of C–H bonds, we identified interactions between the BF_4^- anion and the CH_2 group of the epoxy ring, resulting in blue shifts in the vibrations of CH (SO) and CH_3 (cation). Nevertheless, the spectral results have explained route I in the reaction mechanism, indicating that the IL catalyzes SO first and then reacts with CO_2. Overall, our results provide valuable insights into the underlying mechanism of these reactions.

Supplementary materials: The fitting parameters to the sum frequency spectra of [Bmim][BF_4], styrene oxide, DMF and their binary mixtures, the refractive indices of mixture, tilt angle of DMF-*cis*-CH_3 in [Bmim][BF_4]/DMF mixtures with different R values, and number density and tilt angle of IL-CH_3-ss mode in [Bmim][BF_4]/SO, IL-CH_3-ss mode in [Bmim][BF_4]/DMF, DMF-*cis*-CH_3-ss mode in [Bmim][BF_4]/DMF and DMF-*cis*-CH_3-ss mode in SO/ DMF.

V. NOTES

The authors have no conflicts to disclose.

VI. ACKNOWLEDGEMENTS

This work was supported by the National Natural Science Foundation of China (No.22173112), and Chinese Academy of Sciences (No.YJKYYQ20180014).

[1] L. A. Blanchard, D. Hancu, E. J. Beckman, and J. F. Brennecke, Nature **399**, 28 (1999).
[2] A. P. S. Brogan, L. Bui-Le, and J. P. Hallett, Nat. Chem. **10**, 859 (2018).
[3] X. W. Mao, P. Brown, C. Červinka, G. Hazell, H. Li, Y. Y. Ren, D. Chen, R. Atkin, J. Eastoe, I. Grillo, A. A. H. Padua, M. F. Costa Gomes, and T. A. Hatton, Nat. Mater. **18**, 1350 (2019).
[4] A. Avid, J. L. Ochoa, Y. Huang, Y. C. Liu, P. Atanassov, and I. V. Zenyuk, Nat. Commun. **13**, 6349 (2022).
[5] D. R. MacFarlane, M. Kar, and J. M. Pringle, Weinheim: John Wiley & Sons, (2017).
[6] F. D. Bobbink and P. J. Dyson, J. Catal. **343**, 52 (2016).
[7] J. M. Sun, S. I. Fujita, B. M. Bhanage, and M. Arai, Catal. Commun. **5**, 83 (2004).
[8] W. Chen, L. X. Zhong, X. W. Peng, R. C. Sun, and F. C. Lu, ACS Sustain. Chem. Eng. **3**, 147 (2015).
[9] Z. Ren, A. S. Ivanova, D. Couchot-Vore, and S. Garrett-Roe, J. Phys. Chem. Lett. **5**, 1541 (2014).
[10] A. Kemna and B. Braunschweig, J. Phys. Chem. Lett. **11**, 7116 (2020).
[11] B. Ratschmeier and B. Braunschweig, Electrochem. Sci. Adv. **3**, e2100173 (2023).
[12] K. Motobayashi, Y. Shibamura, and K. Ikeda, Electrochem. Commun. **100**, 117 (2019).
[13] S. Baldelli, J. Phys. Chem. Lett. **4**, 244 (2013).
[14] S. Baldelli, J. M. Bao, W. Wu, and S. S. Pei, Chem. Phys. Lett. **516**, 171 (2011).
[15] G. H. Deng, Y. Q. Guo, X. Li, Z. Zhang, S. L. Liu, Z. Lu, and Y. Guo, Sci. China Chem. **58**, 439 (2015).
[16] Y. R. Shen, Nature **337**, 519 (1989).
[17] Q. Du, R. Superfine, E. Freysz, and Y. R. Shen, Phys. Rev. Lett. **70**, 2313 (1993).
[18] X. D. Zhu, H. Suhr, and Y. R. Shen, Phys. Rev. B **35**, 3047 (1987).
[19] Y. R. Shen, J. Chem. Phys. **153**, 180901 (2020).
[20] R. Lu, W. Gan, B. H. Wu, Z. Zhang, Y. Guo, and H. F. Wang, J. Phys. Chem. B **109**, 14118 (2005).
[21] R. Lu, W. Gan, B. H. Wu, H. Chen, and H. F. Wang, J. Phys. Chem. B **108**, 7297 (2004).
[22] S. Gopalakrishnan, P. Jungwirth, D. J. Tobias, and H. C. Allen, J. Phys. Chem. B **109**, 8861 (2005).
[23] G. H. Deng, X. Li, S. L. Liu, Z. Zhang, Z. Lu, and Y. Guo, J. Phys. Chem. C **120**, 12032 (2016).
[24] Y. N. Zhang, X. J. Qin, X. F. Zhu, M. H. Liu, Y. Guo, and Z. Zhang, Nat. Commun. **13**, 7737 (2022).
[25] E. L. Hommel and H. C. Allen, Analyst **128**, 750 (2003).
[26] T. Kawaguchi, K. Shiratori, Y. Henmi, T. Ishiyama,

DOI: 10.1063/1674-0068/cjcp2401001 © 2024 Chinese Physical Society

and A. Morita, J. Phys. Chem. C **116**, 13169 (2012).
[27] K. Matsuzaki, S. Nihonyanagi, S. Yamaguchi, T. Nagata, and T. Tahara, J. Phys. Chem. Lett. **4**, 1654 (2013).
[28] J. Sung, Y. Jeon, D. Kim, T. Iwahashi, T. Iimori, K. Seki, and Y. Ouchi, Chem. Phys. Lett. **406**, 495 (2005).
[29] S. Rivera-Rubero and S. Baldelli, J. Phys. Chem. B **110**, 15499 (2006).
[30] T. Iwahashi, T. Ishiyama, Y. Sakai, A. Morita, D. Kim, and Y. Ouchi, Phys. Chem. Chem. Phys. **22**, 12565 (2020).
[31] S. Rivera-Rubero and S. Baldelli, J. Phys. Chem. B **110**, 4756 (2006).
[32] C. Romero, H. J. Moore, T. R. Lee, and S. Baldelli, J. Phys. Chem. C **111**, 240 (2007).
[33] C. S. Santos and S. Baldelli, J. Phys. Chem. B **111**, 4715 (2007).
[34] C. S. Santos, S. Rivera-Rubero, S. Dibrov, and S. Baldelli, J. Phys. Chem. C **111**, 7682 (2007).
[35] D. Tomar, B. Rana, and K. C. Jena, J. Chem. Phys. **152**, 114707 (2020).
[36] M. B. Shundalau, P. S. Chybirai, A. I. Komyak, A. P. Zazhogin, M. A. Ksenofontov, and D. S. Umreiko, J. Appl. Spectrosc. **78**, 326 (2011).
[37] M. Sałdyka, Z. Mielke, and K. Haupa, Spectrochim. Acta Part A: Mol. Biomol. Spectrosc. **190**, 423 (2018).
[38] G. R. Bell, C. D. Bain, and R. N. Ward, J. Chem. Soc. Faraday Tran. **92**, 515 (1996).
[39] L. Velarde, X. Y. Zhang, Z. Lu, A. G. Joly, Z. M. Wang, and H. F. Wang, J. Chem. Phys. **135**, 241102 (2011).
[40] R. R. Feng, Y. Guo, and H. F. Wang, J. Chem. Phys. **141**, 18C507 (2014).
[41] X. Zhuang, P. B. Miranda, D. Kim, and Y. R. Shen, Phys. Rev. B **59**, 12632 (1999).
[42] Y. R. Shen, *The Principles of Nonlinear Optics*, New York: John Wiley & Sons, (1984).
[43] A. Pohorille and I. Benjamin, J. Chem. Phys. **94**, 5599 (1991).
[44] F. Matsumura, C. C. Yu, X. Q. Yu, K. Y. Chiang, T. Seki, M. Bonn, and Y. Nagata, J. Phys. Chem. B **127**, 5288 (2023).
[45] C. Romero and S. Baldelli, J. Phys. Chem. B **110**, 6213 (2006).
[46] J. Hou, G. L. Sun, J. C. Liu, X. Gao, X. Y. Zhang, and Z. Lu, J. Phys. Chem. B **124**, 4211 (2020).
[47] Y. L. Yeh, C. Zhang, H. Held, A. M. Mebel, X. Wei, S. H. Lin, and Y. R. Shen, J. Chem. Phys. **114**, 1837 (2001).
[48] H. F. Wang, Prog. Surf. Sci. **91**, 155 (2016).
[49] B. Haddad, D. K. Pandey, D. K. Singh, A. Paolone, M. Drai, D. Villemin, and S. Bresson, Spectrochim. Acta Part A: Mol. Biomol. Spectrosc. **291**, 122325 (2023).
[50] K. Dong, S. J. Zhang, and J. J. Wang, Chem. Commun. **52**, 6744 (2016).
[51] H. F. Wang, W. Gan, R. Lu, Y. Rai, and B. H. Wu, Int. Rev. Phys. Chem. **24**, 191 (2005).
[52] P. B. Petersen and R. J. Saykally, J. Am. Chem. Soc. **127**, 15446 (2005).
[53] A. Castro, K. Bhattacharyya, and K. B. Eisenthal, J. Chem. Phys. **95**, 1310 (1991).
[54] H. Marsh and F. Rodríguez-Reinoso, London: Elsevier, (2006).

DOI: 10.1063/1674-0068/cjcp2401001 © 2024 Chinese Physical Society